Preprints (www.preprints.org) | NOT PEER-REVIEWED | Posted: 24 January 2019 doi:10.20944/preprints201901.0242.v1

Article

First-principles prediction of skyrmionic phase behavior in $GdFe_2$ films capped by 4*d* and 5*d* transition metals

Soyoung Jekal [1,2†],*, Danilo Andreas[3], Dao Phuong[4], and Xiao Zheng[4]

[1] Laboratory of Metal Physics and Technology, Department of Materials, ETH Zurich, 8093 Zurich, Switzerland
[2] Condensed Matter Theory Group, Paul Scherrer Institute, CH-5232 Villigen PSI, Switzerland
[3] Laboratory for Solid State Physics, Department of Physics, ETH Zurich, 8093 Zurich, Switzerland
[4] Hefei National Laboratory, University of Science and Technology of China, Hefei, Anhui 230026, China
* Correspondence: so-young.jekal@mat.ethz.ch; Tel.: +41 44 632 26 43

Abstract: In atomic $GdFe_2$ films capped by 4*d* and 5*d* transition metals, we show that skyrmions with extremely reduced diameters of a smaller than 12 nm can occur. The Dzyaloshinskii-Moriya interaction (DMI), exchange energy, and the magnetocrystalline anisotropy (MCA) energy were investigated based on density functional theory. Since DMI and MCA are caused by spin-orbit coupling, they are increased with 5*d* capping layers compared to films capped by 4*d* transition metal. We discovered a skyrmion phase by using atomistic spin dynamics simulations at small magnetic fields of $\sim$ 1 T. A ground state that a spin spiral phase is remained even at zero magnetic field for both films with 4*d* and 5*d* capping layers.

Keywords: Skyrmion, Dzyaloshinskii–Moriya interaction, exchange energy, magnetic anisotropy

---

1. Introduction

In the sphere of magnetic memory storage especially in spintronics, magnetic skyrmions which is localized topologically protected spin structures are promising candidates due to their unique properties[1–3]. Even though skyrmions have long been widely investigated by simulation works such micromagnetic and phenomenological model calculations[4–6], the experimental discovering of skyrmions was carried out very recently in bulk MnSi.[7] Since then, researchers have focused to make stabilized skyrmions experimentally in not only bulk crystals,[8,9] but also thin films and multilayers[10–14]

At room temperature, Neél-type skyrmions with diameter of $\sim$50 nm are found in multilayer stacks, such as Pt/Co/Ta and Ir/Fe/Co/Pt[15,16]. However, to use them in memory and logic devices, further reduction in skyrmion sizes is inevitable. Problem is that the decreasing stability of small skyrmion at room temperature. Thicker magnetic layers are required to increase stability[17,18]. For multilayer systems consisting ferromagnet and heavy metals, interfacial anisotropy and the strength of Dzyaloshinskii-Moriya interaction (DMI) is getting reduced with increasing thickness of ferromagnetic layer. Moreover, skyrmions Hall effect is challenge on moving skyrmions in electronics devices[19–21]. Amorphous rare-earth-transitional-metal (RE-TM) ferrimagnet is one of the potential materials to overcome these challenges. Their Intrinsic perpendicular magnetocrystalline anisotropy (MCA) gives a advantage in stabilizing skyrmion with using relatively thick magnetic layers ($\approx$5 nm)[22]. Another advantage of RE-TM alloys is that the skyrmion Hall effect is extremely reduced by near zero magnetization of RE-TM alloys[23]. Furthermore, in perspective of the applications, all-optical switching helicity-dependent has been shown in RE-TM alloys due to its ultrafast switching.

© 2019 by the author(s). Distributed under a Creative Commons CC BY license.

Preprints (www.preprints.org) | NOT PEER-REVIEWED | Posted: 24 January 2019 doi:10.20944/preprints201901.0242.v1

Recently, all-optical switching helicity-dependent has been demonstrated in RE-TM alloys using a circularly polarized laser. This is why RE-TM alloys have drawn interest in the field of skyrmions research.

In recent, large skyrmions with diameter of ∼150 nm have been observed in Pt/GdFeCo/MgO[24], and skyrmion bound pairs are found in Gd/Fe multilayers[25]. However, further tuning is essential to reduce the size of skyrmion in RE-TM alloys.

In present paper, magnetic properties such as DMI, MCA, and magnetic phase transition are investigated in an atomic $GdFe_2$ capped by 4*d* and 5*d* transition metals (TMs) films using a first principles density functional theory (DFT) and atomistic spin dynamics. We recognized that the 5*d* TMs gave rise to a large DMI and strong MCA due to their large spin-orbit coupling (SOC) and orbital hybridization with 3*d* of Fe atom. First, by using atomistic spin dynamics, an extended Heisenberg model is studied. Then, we parameterize an extended Heisenberg model from DFT calculations. According to phase diagram which observed at zero temperature, there are phase transitions occur under externally applied magnetic fields on the order of ∼1 T. When phase changes from the spin spiral state to the ferromagnetic state via skyrmion lattice, the skyrmion diameters of isolated skyrmions amount to 6 to 15 nm depending on the capping layers.

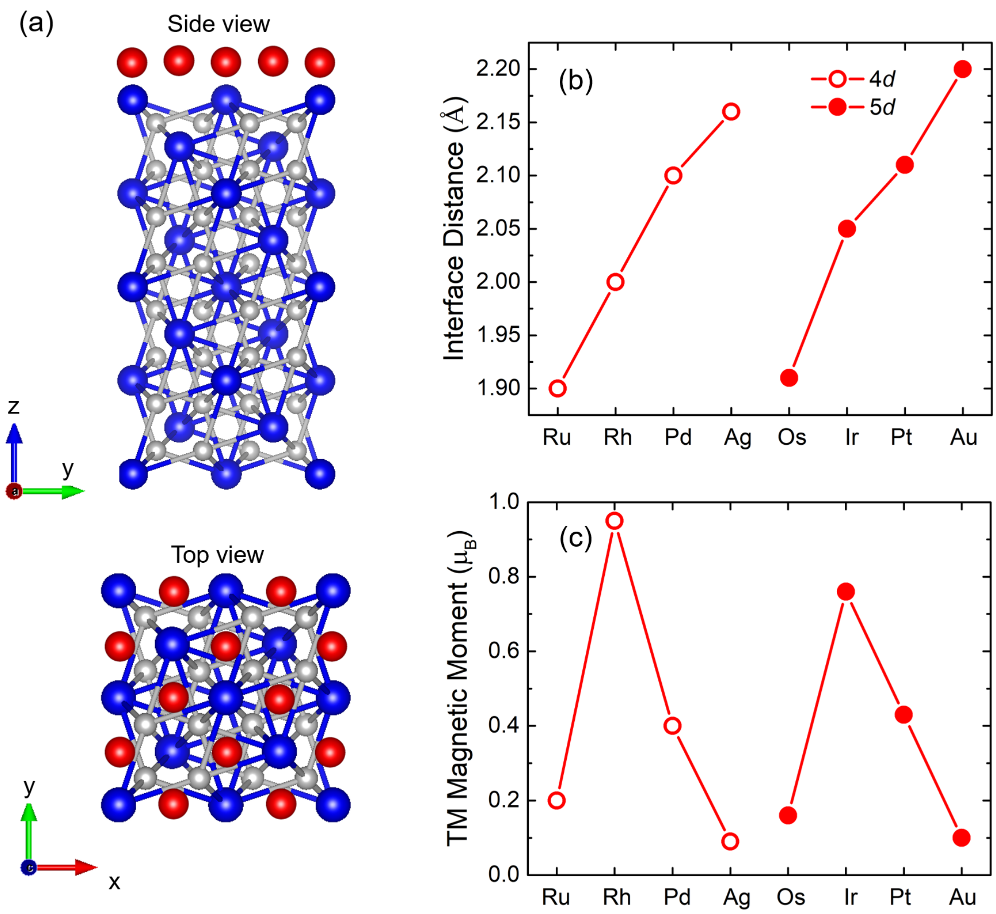

Figure 1. (a) Side view and top view of $GeFe_2$ film capped by one TM layer. Blue, gray, and red balls represent Gd, Fe, and TM atoms, respectively. TM atoms are on the hollow site of $GeFe_2$. (b) Interface distances between the TM capping layer and $GeFe_2$ after structural optimization. (c) Magnetic moments of TM atoms, induced by $GeFe_2$.

Preprints (www.preprints.org) | NOT PEER-REVIEWED | Posted: 24 January 2019 doi:10.20944/preprints201901.0242.v1

2. Methods

We have used DFT as implemented in the Quantum Espresso[26] and Fleur code[27] to investigate the electronic and magnetic properties of $GdFe_2$/TMs film. For the TMs capping layers, we have considered Ru, Rh, Pd, and Ag in 4*d* and Os, Ir, Pt and Au in 5*d*. For the exchange-correlation potential we adapted the generalized gradient approximation (GGA). The wave functions were expanded by a plane-wave basis set with an optimized cutoff energy of 350 Ry, and the Brillouin zone was sampled via a $12 \times 12 \times 1$ *k*-point mesh. Different mesh values from 36 to 256 were tested to ensure the precise of our calculations, with the convergence criterion being 0.1 eV. The convergence with respect to cutoff was also carefully checked.

Total energy E(q) is calculated along the paths of $\bar{\Gamma}$-$\bar{K}$ and $\bar{\Gamma}$-$\bar{M}$ which have the highest symmetry among other directions in the two-dimensional Brillouin zone (2D BZ). E(q) with and without SOC[28] are seprately displayed in Fig. 3. In the 2D BZ, we characterize spin spiral phase by using the wave vector $\mathbf{q}$ with a constant angle of ϕ, where ϕ is defined as $\mathbf{q}\cdot\mathbf{R}$.

In order to examine the magnetically characteristic of $GdFe_2$ films with TM cappings, we adopt the atomistic spin model described as[29–31]

$$H = -\sum_{ij} J_{ij}(m_i \cdot m_j) - \sum_{ij} D_{ij}(m_i \times m_j) + \sum_i K(m_i^z)^2 - \sum_i \mu_s(B_i). \tag{1}$$

By using Eq. (1), we can describe the magnetic interactions between two neighbor Fe atoms with spins of $\mathbf{M}_i$ and $\mathbf{M}_j$ at sites $\mathbf{R}_i$ and $\mathbf{R}_j$, respectively. Here, m_i is defined as $\mathbf{M}_i/\mu_s$. For both energy dispersion curves without and with SOC are calculated and fitted to extract the parameters for the exchange interactions (J_{ij}) and the DMI (D_{ij}).

The MCA energy was calculated using the force theorem and defined as the total energy difference between the magnetization perpendicular to the [100]-plane and parallel to the [100]-plane. Therefore, MCA energy E_{MCA}= $\text{E}_{[100]} - E_{[001]}$, where $E_{[100]}$ and $E_{[001]}$ are the total energies with the magnetization aligned along the [100] and [001] of the magnetic anisotropy, respectively.

3. Results and discussions

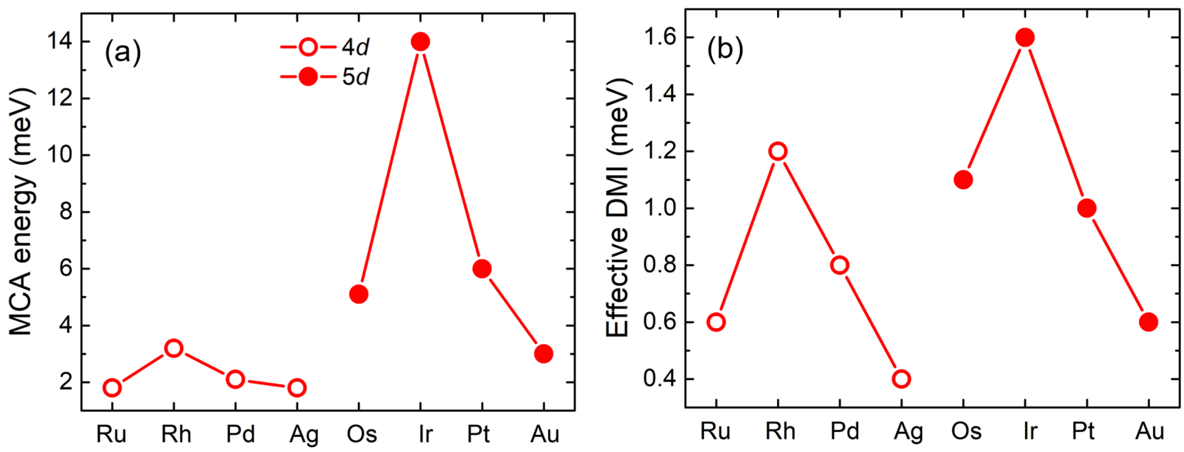

Figure 2. (a)Total MCA energy and (b) Effective DMI of $GdFe_2$ with TM capping layer.

The in-plane lattice constant of 7.32 Å was taken from the experimental lattice constant of laves phase of $GdFe_2$, with lattice mismatches of 3.6% (Rh)–14.2% (Os), as depicted in Fig. 1(a). From the total energy calculation, it was confirmed that the hollow site is the most energetically favorable to stack TM layer (see Fig.1). The atoms of $GdFe_2$ and TM capping layer were fully relaxed by atomic force calculations.

Preprints (www.preprints.org) | NOT PEER-REVIEWED | Posted: 24 January 2019 doi:10.20944/preprints201901.0242.v1

After structural optimization, the interface distances between TM capping layer and the $GdFe_2$ is presented in Fig.1(b). As the atomic number becomes larger in the 4d and 5d TMs , the interlayer distances increase monotonically. Induced spin moments of the TMs for TM/$GdFe_2$ are presented in Figs.1(c). Rh and Ir capping layers, which are the Co-group elements are found to have the largest moments of 0.98 and 0.80 μ_B. For all of the TM/$GdFe_2$, the direction of magnetization is favored to perpendicularly orientate to the film plane. Interestingly, the MCA energy and DMI of $GdFe_2$ films capped by 5*d* TMs are significantly larger than those of $GdFe_2$ with 4*d* TMs. In particular, the Ir-capped $GdFe_2$ film exhibits the largest MCA energy of 14.1 meV and effective DMI of 1.6 meV. We attribute the substantial enhancement of MCA energy and DMI in $GdFe_2$ with 5*d* capping layer to the strong SOC of the 5*d* orbitals because the SOC is proportional to the fourth power of the atomic number. Since the 4*d* also exhibit similar trend with 5*d*, e.g. Rh and Ir have the largest magnetic moments and MCA energy, this is related to the band-filling effect orbital hybridization.

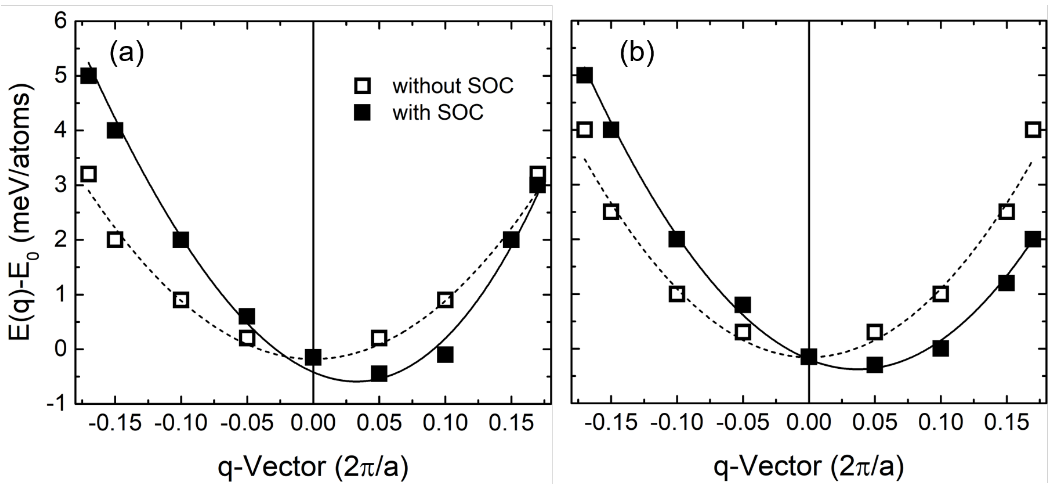

Figure 3. Energy dispersion E(q) of homogeneous cycloidal flat spin spirals in high-symmetry direction $\bar{\Gamma}$-$\bar{K}$ for (a)$GdFe_2$/Rh and (b) $GdFe_2$/Rh films. Filled and empty symbols represent E(q) with and without SOC, respectively. The energy is given relative to the magnetic ground state. The dispersion is fitted to the Heisenberg model (dotted line) and includes the DMI and MCA (solid line).

The calculated energy dispersion E(q) of spin spirals is presented in Fig.3 along the high-symmetry direction, $\bar{\Gamma}$-$\bar{K}$ for $GdFe_2$ capped by Rh and Ir which exhibit the largest magnetic moment, MCA energy, and effective DMI among the 4*d* and 5*d* element, respectively. For results without SOC, a minimum point of the energy dispersion is observed at the $\bar{\Gamma}$ point, and it degenerates for right-(q > 0) and left-rotating (q < 0) spirals. For both Rh and Ir stackings, it is confirmed that the out-of-plane direction is an easy magnetization axis due to SOC (see Fig.2(a)). Due the imperfect inversion symmetry at the interface, the SOC for spin spirals derives DMI in system[32,33]. Therefore, DMI leads to non-collinear spin structures with the magnetic moments on an oblique angle. In case of the inclusion of the DMI, the E(q) has the lowest value for a homogeneous cycloidal flat spin spiral state with a particular rotational sense[34]. As presented in Fig.3, an energy minimum of 0.50 meV/atom and 0.35 meV/atom compared to the ground magnetic state appears for a right rotating spin spiral for $GdFe_2$ films with Rh and Ir capping, respectively.

To investigate the magnetic phase transitions in $GdFe_2$/Rh and $GdFe_2$/Ir under the external magnetic field at 0 K, we have performed atomistic spin-dynamics simulations using the model described by Eq. (1). Using the parameters obtained from DFT, the magnetic phase diagrams is displayed in Fig.4(a) and (b). At zero applied magnetic field, the ground magnetic state is a spin spiral consistent with the energy minimum. For film capped by Rh, the skyrmion lattice is energetically stable at a critical field value of $\sim$ 1.12 T, and this skyrmion lattice phase is changed to the ferromagnetic phase by a larger critical field value of $\sim$ 2.25 T. For film capped by Ir, the skyrmion lattice emerge at relatively weak field of 0.75 T, and disappear for a large filed of $\sim$ 1.74 T.

Preprints (www.preprints.org) | NOT PEER-REVIEWED | Posted: 24 January 2019 doi:10.20944/preprints201901.0242.v1

In our simulation, the spin structure is relaxed using spin dynamics. As shown in Fig.4(c), for both Rh and Ir capped $GdFe_2$, skyrmions with diameter of $\sim$ 2–4 nm emerge under external magnetic fields of 1–2 T. The size of skyrmion decrease rapidly with increasing value of applied magnetic field. For deeper insights into the skyrmion size, the diameter has been computed for isolated single skyrmions via two different ways; (i) using the fixed MCA energy and exchange constants obtained from DFT calculation but varying the DMI value, (ii) using fixed DMI obtained from DFT but varying the MCA. From these calculations we confirmed that the skyrmion size decreases with reduced DMI but it expands with reduced MCA.

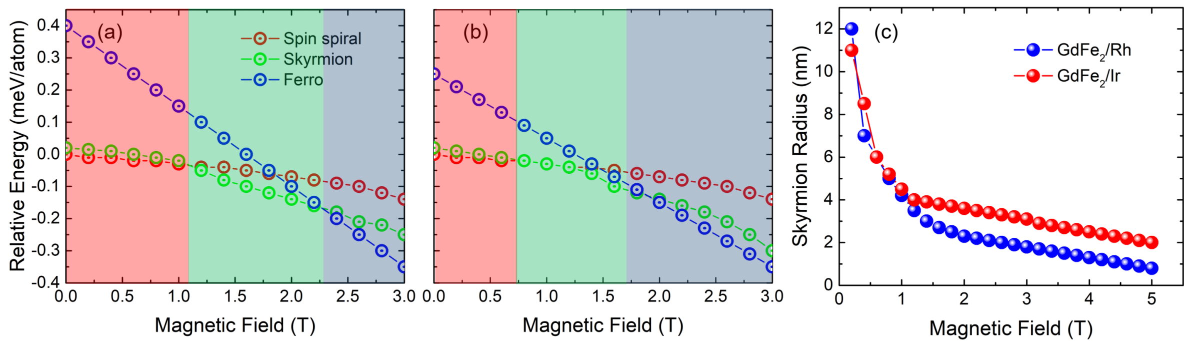

Figure 4. Phase diagram for (a)$GdFe_2$/Rh and (b)$GdFe_2$/Ir at zero temperature. The relative energies of the spin spiral states, skyrmion lattice, and ferromagnetic state are shown. Red, green, and blue color represents the regime of the spin spiral states, skyrmion lattice, and ferromagnetic state, respectively. (c)Radii of skyrmions in the films of $GdFe_2$/Rh and $GdFe_2$/Ir as a function of the applied magnetic field.

4. Conclusion

The creation of isolated and stabilized skyrmions with an extremely reduced sizes of a only few nanometers in $GdFe_2$ films can be predicted by 4 and 5*d* TMs capping. While behavior of the atomistic spin model was studied by spin dynamics simulations, first-principles parameters were obtained from density functional theory calculation. For future experimental work, this simulation work guides us to explore novel skyrmion systems.

1. Fert, A.; Cros, V.; Sampaio, J. Skyrmions on the track. *Nature nanotechnology* **2013**, *8*, 152.
2. Wiesendanger, R. Nanoscale magnetic skyrmions in metallic films and multilayers: a new twist for spintronics. *Nature Reviews Materials* **2016**, *1*, 16044.
3. Kiselev, N.; Bogdanov, A.; Schäfer, R.; Rößler, U. Chiral skyrmions in thin magnetic films: new objects for magnetic storage technologies? *Journal of Physics D: Applied Physics* **2011**, *44*, 392001.
4. Bogdanov, A.; others. AN Bogdanov and DA Yablonskii, Sov. Phys. JETP 68, 101 (1989). *Sov. Phys. JETP* **1989**, *68*, 101.
5. Bogdanov, A.; Hubert, A. Thermodynamically stable magnetic vortex states in magnetic crystals. *Journal of magnetism and magnetic materials* **1994**, *138*, 255–269.
6. Bogdanov, A.; Rößler, U. Chiral symmetry breaking in magnetic thin films and multilayers. *Physical review letters* **2001**, *87*, 037203.
7. Mühlbauer, S. S. Mühlbauer, B. Binz, F. Jonietz, C. Pfleiderer, A. Rosch, A. Neubauer, R. Georgii, and P. Böni, Science 323, 915 (2009). *Science* **2009**, *323*, 915.
8. Wilhelm, H.; Baenitz, M.; Schmidt, M.; Rößler, U.; Leonov, A.; Bogdanov, A. Precursor phenomena at the magnetic ordering of the cubic helimagnet FeGe. *Physical review letters* **2011**, *107*, 127203.
9. Münzer, W.; Neubauer, A.; Adams, T.; Mühlbauer, S.; Franz, C.; Jonietz, F.; Georgii, R.; Böni, P.; Pedersen, B.; Schmidt, M.; others. Skyrmion lattice in the doped semiconductor $Fe_{1-x}Co_xSi. Physical Review B$ **2010**, 81, 041203.

Preprints (www.preprints.org) | NOT PEER-REVIEWED | Posted: 24 January 2019 doi:10.20944/preprints201901.0242.v1

10. Yu, X. XZ Yu, N. Kanazawa, Y. Onose, K. Kimoto, WZ Zhang, S. Ishiwata, Y. Matsui, and Y. Tokura, Nat. Mater. 10, 106 (2011). *Nat. Mater.* **2011**, *10*, 106.
11. Tonomura, A.; Yu, X.; Yanagisawa, K.; Matsuda, T.; Onose, Y.; Kanazawa, N.; Park, H.S.; Tokura, Y. Real-space observation of skyrmion lattice in helimagnet MnSi thin samples. *Nano letters* **2012**, *12*, 1673–1677.
12. Heinze, S.; Von Bergmann, K.; Menzel, M.; Brede, J.; Kubetzka, A.; Wiesendanger, R.; Bihlmayer, G.; Blügel, S. Spontaneous atomic-scale magnetic skyrmion lattice in two dimensions. *Nature Physics* **2011**, *7*, 713.
13. Romming, N.; Hanneken, C.; Menzel, M.; Bickel, J.E.; Wolter, B.; von Bergmann, K.; Kubetzka, A.; Wiesendanger, R. Writing and deleting single magnetic skyrmions. *Science* **2013**, *341*, 636–639.
14. Romming, N.; Kubetzka, A.; Hanneken, C.; von Bergmann, K.; Wiesendanger, R. Field-dependent size and shape of single magnetic skyrmions. *Physical review letters* **2015**, *114*, 177203.
15. Woo, S.; Litzius, K.; Krüger, B.; Im, M.Y.; Caretta, L.; Richter, K.; Mann, M.; Krone, A.; Reeve, R.M.; Weigand, M.; others. Observation of room-temperature magnetic skyrmions and their current-driven dynamics in ultrathin metallic ferromagnets. *Nature materials* **2016**, *15*, 501.
16. Soumyanarayanan, A.; Raju, M.; Oyarce, A.G.; Tan, A.K.; Im, M.Y.; Petrović, A.P.; Ho, P.; Khoo, K.; Tran, M.; Gan, C.; others. Tunable room-temperature magnetic skyrmions in Ir/Fe/Co/Pt multilayers. *Nature materials* **2017**, *16*, 898.
17. Siemens, A.; Zhang, Y.; Hagemeister, J.; Vedmedenko, E.; Wiesendanger, R. Minimal radius of magnetic skyrmions: statics and dynamics. *New Journal of Physics* **2016**, *18*, 045021.
18. Büttner, F.; Lemesh, I.; Beach, G.S. Theory of isolated magnetic skyrmions: From fundamentals to room temperature applications. *Scientific reports* **2018**, *8*, 4464.
19. Jiang, W.; Zhang, X.; Yu, G.; Zhang, W.; Wang, X.; Jungfleisch, M.B.; Pearson, J.E.; Cheng, X.; Heinonen, O.; Wang, K.L.; others. Direct observation of the skyrmion Hall effect. *Nature Physics* **2017**, *13*, 162.
20. Litzius, K.; Lemesh, I.; Krüger, B.; Bassirian, P.; Caretta, L.; Richter, K.; Büttner, F.; Sato, K.; Tretiakov, O.A.; Förster, J.; others. Skyrmion Hall effect revealed by direct time-resolved X-ray microscopy. *Nature Physics* **2017**, *13*, 170.
21. Tomasello, R.; Martinez, E.; Zivieri, R.; Torres, L.; Carpentieri, M.; Finocchio, G. A strategy for the design of skyrmion racetrack memories. *Scientific reports* **2014**, *4*, 6784.
22. Harris, V.G.; Pokhil, T. Selective-resputtering-induced perpendicular magnetic anisotropy in amorphous TbFe films. *Physical review letters* **2001**, *87*, 067207.
23. Hansen, P.; Clausen, C.; Much, G.; Rosenkranz, M.; Witter, K. Magnetic and magneto-optical properties of rare-earth transition-metal alloys containing Gd, Tb, Fe, Co. *Journal of applied physics* **1989**, *66*, 756–767.
24. Woo, S.; Song, K.M.; Zhang, X.; Zhou, Y.; Ezawa, M.; Liu, X.; Finizio, S.; Raabe, J.; Lee, N.J.; Kim, S.I.; others. Current-driven dynamics and inhibition of the skyrmion Hall effect of ferrimagnetic skyrmions in GdFeCo films. *Nature communications* **2018**, *9*, 959.
25. Lee, J.T.; Chess, J.; Montoya, S.; Shi, X.; Tamura, N.; Mishra, S.; Fischer, P.; McMorran, B.; Sinha, S.; Fullerton, E.; others. Synthesizing skyrmion bound pairs in Fe-Gd thin films. *Applied Physics Letters* **2016**, *109*, 022402.
26. Giannozzi, P.; et al.. QUANTUM ESPRESSO: a modular and open-source software project for quantum simulations of materials. *Journal of physics: Condensed matter* **2009**, *21*, 395502.
27. Wimmer, E. E. Wimmer, H. Krakauer, M. Weinert, and AJ Freeman, Phys. Rev. B 24, 864 (1981). *Phys. Rev. B* **1981**, *24*, 864.
28. Kurz, P.; Förster, F.; Nordström, L.; Bihlmayer, G.; Blügel, S. Ab initio treatment of noncollinear magnets with the full-potential linearized augmented plane wave method. *Physical Review B* **2004**, *69*, 024415.
29. Eriksson, O.; Bergman, A.; Bergqvist, L.; Hellsvik, J. *Atomistic spin dynamics: foundations and applications*; Oxford university press, 2017.
30. Antropov, V. VP Antropov, MI Katsnelson, BN Harmon, M. van Schilfgaarde, and D. Kusnezov, Phys. Rev. B 54, 1019 (1996). *Phys. Rev. B* **1996**, *54*, 1019.
31. Katsnelson, M. MI Katsnelson, V. Yu. Irkhin, L. Chioncel, AI Lichtenstein, and RA de Groot, Rev. Mod. Phys. 80, 315 (2008). *Rev. Mod. Phys.* **2008**, *80*, 315.
32. Dzyaloshinskii, I. IE Dzyaloshinskii, Sov. Phys. JETP 5, 1259 (1957). *Sov. Phys. JETP* **1957**, *5*, 1259.
33. Moriya, T. New mechanism of anisotropic superexchange interaction. *Physical Review Letters* **1960**, *4*, 228.
34. Bode, M.; Heide, M.; Von Bergmann, K.; Ferriani, P.; Heinze, S.; Bihlmayer, G.; Kubetzka, A.; Pietzsch, O.; Blügel, S.; Wiesendanger, R. Chiral magnetic order at surfaces driven by inversion asymmetry. *Nature* **2007**, *447*, 190.